Biosensors and Bioelectronics 52 (2014) 129–135

Contents lists available at ScienceDirect

Biosensors and Bioelectronics

journal homepage: www.elsevier.com/locate/bios

Sub-femtomole detection of 16s rRNA from *Legionella pneumophila* using surface plasmon resonance imaging

Amir M. Foudeh [a,1], Jamal T. Daoud [a,1], Sebastien P. Faucher [c,2], Teodor Veres [a,d,3], Maryam Tabrizian [a,b,*,1]

[a] Department of Biomedical Engineering, Faculty of Medicine, McGill University, Montreal, Canada
[b] Faculty of Dentistry, McGill University, Strathcona Anatomy & Dentistry Building 3640 University Street Montreal, Quebec, Canada
[c] Department of Natural Resource Sciences, McGill University, Quebec, Canada
[d] National Research Council of Canada, Quebec, Boucherville, Canada

ARTICLE INFO

Article history:
Received 9 July 2013
Received in revised form
16 August 2013
Accepted 19 August 2013
Available online 28 August 2013

Keywords:
Legionella pneumophila
Surface plasmon resonance imaging
Pathogen detection
16s rRNA
Quantum dot
Hybridization

ABSTRACT

Legionellosis has been and continues to be a life-threatening disease worldwide, even in developed countries. Given the severity and unpredictability of Legionellosis outbreaks, developing a rapid, highly specific, and sensitive detection method is thus of great pertinence. In this paper, we demonstrate that sub-femtomole levels of 16s rRNA from pathogenic *Legionella pneumophila* can be timely and effectively detected using an appropriate designed capture, detector probes, and a QD SPRi signal amplification strategy. To achieve specific and sensitive detection, optimal hybridization conditions and parameters were implemented. Among these parameters, fragmentation of the 16s rRNA and further signal amplification by QDs were found to be the main parameters contributing to signal enhancement. The appropriate design of the detector probes also increased the sensitivity of the detection system, mainly due to secondary structure of 16s rRNA. The use of 16s rRNA from *L. pneumophila* allowed for the detection of metabolically active pathogens with high sensitivity. Detection of 16s rRNA in solutions as diluted as 1 pM at 450 μL (0.45 femtomole) was achieved in less than 3 h, making our approach suitable for the direct, timely, and effective detection of *L. pneumophila* within man-made water systems.

1. Introduction

Legionellosis is an acute form of pneumonia and Pontiac fever, a milder form of the disease with flu-like symptoms (Swanson and Hammer, 2000) that has been and continues to be devastating worldwide, even in developed countries. This is mainly attributed to unpredictable outbreaks, such as recent incidents reported in Canada, the U.S.A., Norway, and Germany (CDC, 2011; Nygård et al., 2008; Von Baum et al., 2010). *Legionella pneumophila* is the causative agent of Legionellosis. The fatality rate of Legionellosis ranges between 10% and 40% and approaches 50% within hospital and industrial outbreak settings, particularly affecting individuals with compromised health status (Swanson and Hammer, 2000). *L. pneumophila* is found in most natural and engineered water systems, where it contaminates and multiplies inside ameba (Wadowsky et al., 1991). The literature indicates that modern water systems, such as air-conditioning units, showers, and industrial refrigeration towers provide optimal growth conditions for *L. pneumophila* and propagate its transmission through aerosol (WHO, 2003). Transmission to the human host thus occurs through the inhalation of contaminated water droplets. Once in the lungs, *L. pneumophila* infects and replicates inside alveolar macrophages and causes widespread tissue damage (Swanson and Hammer, 2000).

Current conventional detection methods include identification via laboratory culture and polymerase chain reaction (PCR) (Foudeh et al., 2012; Lazcka et al., 2007). Laboratory culture is the gold standard method employed to detect *L. pneumophila*. However, laboratory culture suffers from low sensitivity, especially if the samples under study contain microorganisms that inhibit *Legionella's* growth. Another drawback is its inability to detect

* Corresponding author at: Department of Biomedical Engineering, Faculty of Medicine, McGill University, Montreal, Canada. Tel.: +1 514 398 8129; fax: +1 514 398 7461.
E-mail addresses: amir.foudeh@mail.mcgill.ca (A.M. Foudeh), jamal.daoud@mail.mcgill.ca (J.T. Daoud), sebastien.faucher2@mcgill.ca (S.P. Faucher), Teodor.Veres@cnrc-nrc.gc.ca (T. Veres), maryam.tabrizian@mcgill.ca (M. Tabrizian).
[1] 3775 University Street, Department of Biomedical Engineering, Faculty of Medicine, McGill University, Montreal (QC), Canada H3A 2B4. Tel.: +1 514 398 3469; fax: +1 514 398 7469.
[2] Department of Natural Resource Sciences, Macdonald Campus, 12 McGill University, 21,111 Lakeshore, Ste-Anne-de-Bellevue, Quebec, H9X 3V9. Tel.: +1 514 398 13 7886; fax: +1 514 398 7990.
[3] National Research Council Canada, 75 Boul. de Mortagne Boucherville, QC, Canada J4B 6Y4. Tel: +1 450 641 5232; fax: +1 450 641 5105.

0956-5663/$ - see front matter © 2013 Elsevier B.V. All rights reserved.
http://dx.doi.org/10.1016/j.bios.2013.08.032

viable but non-culturable *Legionella* even though they might potentially be pathogenic. While laboratory culture entails long procedures requiring several days, PCR is a faster detection methodology and highly specific. However, it is laborious and normally requires centralized laboratory facilities. PCR is especially unreliable when analyzing environmental samples due to the presence of PCR inhibitors.

Other methods, namely antibody-based detection, have also been investigated (Oh et al., 2003). This method is fairly rapid, but cross-reactivity between species is an important shortcoming that limits the specificity of the technique. DNA/PNA microarray-based detection targeting DNA in bacteria is another alternative that provides the desired specificity by targeting species-specific sequences in DNA (Zhou et al., 2011).

The main drawback of all the aforementioned methods is their inability to differentiate between live and dead bacterial cells, which is critical for achieving accurate and reliable results.

To overcome the limitations of using DNA and antigen targeting-based techniques, detection of the bacterial RNA is a viable alternative approach. The presence of RNA in bacteria is directly correlated with microbial activity since, following bacterial death, the associated RNA degrades relatively rapidly (McKillip et al., 1998), further enhancing the associated accuracy and reliability of bacterial detection. Among RNA types, 16s rRNA is highly conserved between different species of bacteria and has been utilized for microbial identification (Clarridge, 2004; Coenye and Vandamme, 2003). The presence of high copy numbers of 16s rRNA in each bacterium is another motivation to identify bacteria through the direct detection of 16s rRNA. However, instability and the presence of a secondary structure are significant drawbacks of using ribosomal RNA. The secondary structure renders access to the target sequence difficult. This is why methods such as using multiple adjunct probes, heat denaturation, and fragmentation have been used to circumvent this issue (Hwang et al., 2011; Small et al., 2001).

Focusing on the detection of 16s rRNA, various sensing techniques, including electrochemical sensors (Bockisch et al., 2005; Xie et al., 2004), impedance (Elsholz et al., 2006), fluorescent microscopy (Gerasimova and Kolpashchikov, 2012; Hwang et al., 2011; Riahi et al., 2011), surface-enhanced Raman spectroscopy (SERS) (Stephen et al., 2012), and surface plasmon resonance (SPR) (Joung et al., 2008; Small et al., 2001) were used for bacterial species-specific detection. Among these methods, SPR imaging (SPRi) has proven to be a versatile tool for the real-time study of genomic and proteomic interactions and kinetics. In contrast to classical wavelength or scanning angle SPR systems, SPRi provides visualization of the multiple interactions simultaneously in real time thanks to the integration of a charge-coupled device (CCD) camera with the associated sensogram. In contrast to other end-point measurement systems, the use of SPRi allows detailed kinetic analysis, monitored in real time, to elucidate analyte binding behavior further, as well as to differentiate better between specific and non-specific adsorptions. To date, few reports on detecting 16s rRNA within a SPR setup are available in the literature. Nelson et al. detected 16s rRNA from *E. coli* with a limit of detection (LOD) of 2 nM through the use of DNA probes (Nelson et al., 2000). Joung et al. used PNA probes and electrostatic interaction between positively charged gold nanoparticles and negatively charged RNA as a signal post amplification method, achieving an LOD of around 100 pM (Joung et al., 2008), which is far from the desired sensitivity in the context of the detection of pathogenic *L. pneumophila* in a water sample.

This work presents the first report on utilizing 16s rRNA for the detection of *L. pneumophila* with SPRi. To overcome the lack of desired SPRi sensitivity for the detection of this species, near-infrared quantum dots (QDs) are employed as a post-amplification strategy. We previously demonstrated that QDs with an emission of 800 nm induce the strongest SPR signal enhancement among QDs with differing wavelengths (Malic et al., 2011). As such, our aim was to address the main challenges associated with the detection of *L. pneumophila* through the use of 16s rRNA from *L. pneumophila*, allowing for the detection of only metabolically active pathogens with high sensitivity. With the design of two probes, one to capture the RNA on the substrate and the other to increase the detection sensitivity, for each target region, the high specificity of the detection system is further ensured (Scheme 1). The effect of experimental parameters, including temperature, buffer composition, length of the spacer between the detector probe and the biotin, and the pre-treatment of 16s rRNA were investigated and optimized to reach a sensitivity detection of *L. pneumophila* in the femtomole range.

2. Materials and methods

2.1. Chemical and reagents

6-Mercapto-1-hexanol(MCH), potassium phosphate dibasic solution, 1 M, pH 8.9 (1 M K_2HPO_4), sodium chloride (NaCl), sodium hydroxide (NaOH), sulfuric acid (H_2SO_4), hydrogen peroxide (H_2O_2), and ethanol were purchased from Sigma-Aldrich (St. Louis, MO,U.S.A.). A fragmentation kit was obtained from Ambion. Oligonucleotides (ODN) were purchased from Integrated DNA Technologies (Coralville, IA, U.S.A.). Streptavidin-coated quantum dots, Qdot 800 STVD, SSPE buffer (20 × buffer is 3.0 M NaCl, 0.2 M NaH_2PO_4, and 0.02 M EDTA at pH 7.4.), and Denhardt's solution [50 × solution is 1% Ficoll (type 400), 1% polyvinylpyrrolidone, and 1% bovine serum albumin] were purchased from Invitrogen (Carlsbad, CA, U.S.A.).

2.2. DNA probe design

Two specific DNA capture probes (CP), referring to leg1 CP and leg2 CP, complementary to *L. pneumophila's* 16s rRNA, were designed using bioinformatics software packages from Cardiff University, England. Particular features in the sequence, such as loops and hairpin curves, were checked and avoided. The specificity of these probes was confirmed by submitting the sequence to the Check Probe program of the Ribosomal Database Project (RDP). In terms of detection probes, two different biotinylated probes with gap of 0 bp and 7 bp (Leg1 DP 0/7 bp and Leg2 DP 0/7 bp) between the capture and detection probes for each target RNA sequence were designed. Finally, a DNA probe and a universal probe (EU capture probe) were used as negative and positive controls, respectively. The length of each detector probe was determined to ensure similar melting temperatures while avoiding cross-reactivity and hybridization to any capture probes. This was verified by including a detector-only control for each hybridization experiment conducted (data not shown). The secondary structure model of *L. pneumophila* was obtained from http://www.rna.ccbb.utexas.edu(Cannone et al., 2002).

2.3. RNA preparation

Synthetic 60 bp RNA from the *L. pneumophila's* 16s rRNA, which contains complementary sequences for Leg1 capture and detector probes, was synthesized by Integrated DNA Technology Table S1. Moreover, 16s rRNA of *L. pneumophila* was produced using T7 RNA polymerase-driven in vitro synthesis methodology. Briefly, the 16s rRNA gene of *L. pneumophila* was amplified by PCR from DNA extracted from *L. pneumophila* using specific primers (5'-AGACAAAC-TGTGTGGGCACTTTGG-3' and 5'-TGGGCACTTTGATTCCTTCTGTGC-3'). The PCR fragment was then inserted into the pGEM-T (Promega)

vector downstream of the T7 promoter. The plasmid was then transformed and propagated in JM109 high-efficiency competent cells. The PCR fragments could become inserted in the sense or antisense orientation. Plasmids carrying fragments in the sense orientation were identified and utilized for further experiments. The identification of colonies carrying plasmids containing fragments in each orientation were identified by PCR, and the correct sequence of the fragment was validated by sequencing. The plasmids carrying the correct sequences were isolated and used as a template for T7 RNA polymerase (New England Biolabs) to produce 16s rRNA. The resulting RNA product was further purified by acid-phenol and stored in −80 °C for further use.

2.4. Surface chemistry on SPRi chip

Gold-coated slides (Horiba, France) were cleaned with UV/ozone for 10 min, rinsed thoroughly with MQ water, and treated with piranha solution for another 5 min. After rinsing with MQ water, the slides were dried under a stream of nitrogen. DNA immobilization was performed using 1 μM thiol-modified oligonucleotide probes comprising a 10T spacer in 1 M KH_2PO_4 for 180 min. Following the immobilization, substrates were treated with 1 mM MCH for 90 min to improve the orientation of the probes and attenuate non-specific adsorption. The slides were further passivated with 2.5X Denhardt solution for 10 min and stored at 4 °C before further use.

2.5. RNA pre-treatment

Denaturation of the 16s rRNA was carried out by the incubation of samples in 65 °C for 5 min. Fragmentation of the 16s rRNA was performed according to the protocol provided by the manufacturer (Ambion) except that different concentrations of the fragmentation buffer (zinc solution) were used in these experiments. Frag1 and Frag2 represent the use of 1 and 2 μL of the fragmentation buffer, respectively. Then the solution was mixed with 1.28 μg of 16s rRNA in 20 μL of total reaction volume. The solution was kept at 75 °C for 15 min, followed by the addition of blocking solution (EDTA). The samples were kept on ice until further use.

2.6. SPRi measurements

SPRi detection of biomolecular binding to the chip surface was performed using a scanning-angle SPRi instrument (model SPRi-Lab+, GenOptics, France). The SPRi apparatus, equipped with an 800 nm LED source, a CCD camera, and a microfluidic cell, was placed in an incubator (Memmert Peltier, Rose Scientific, Canada). The SPRi measurements for each spot were taken as described previously (Malic et al., 2011). The entire biochip surface was imaged during the angular scan. At least five spots were selected for each experiment to monitor the binding events with both the probes and the controls, and each experiment was repeated at least three times.

RNA hybridization experiments were carried at 37 °C with an injection volume of 450 μL. A baseline signal was first obtained for the hybridization buffer, followed by the hybridization signal for the targets. Detector probes were pre-mixed with the RNA samples before injection. Following the hybridization of the target RNA with the capture probe and the detection probe, streptavidin-conjugated Qdots (SA-QDs), 1 nM in concentration in hybridization buffer, were injected and allowed to bind to the biotinylated detector probes for 10 min. At each step, the substrate was washed with buffer, and the difference in the reflected intensity ($\Delta\%R$) was computed by taking the difference between the initial and final buffer signals. Successive hybridizations were followed by surface regeneration using 50 mM NaOH, without significant binding efficiency loss.

2.7. Statistics

The lower detection limit was defined as the smallest concentration of an analyte, calculated as the blank signal plus or minus three standard deviations. All data were expressed as the mean ± SD. Statistical comparisons between two groups were done using Student's paired *t*-test, while multiple comparisons were done using one-way ANOVA, followed by the post hoc Tukey test.

3. Results and discussion

Two different regions of the *L.pneumophila*'s 16s rRNA sequence were targeted to investigate the regional effects on hybridization

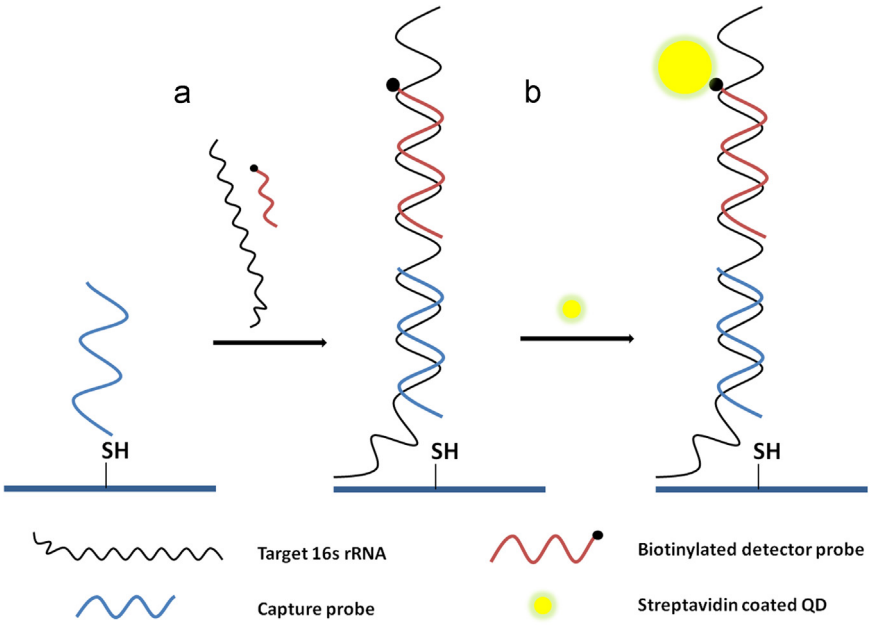

Scheme 1. . Schematic illustration of the RNA hybridization using capture and detector probes, before and after addition of SA-QDs. (a) Mixture of target RNA and biotinylated detector probe pass through the detection surface. (b) Addition of streptavidin-QDs after hybridization of target RNA to capture probe and detector probe.

efficiency and specificity, as well as the proximity of the detector and capture probes. One specific capture probe was designed for each region. In addition to these two specific capture probes for *L. pneumophila*, one universal probe and one control probe were selected as positive and negative controls, respectively. A summary of the oligonucleotide sequences for probes are given in Table S1.

Since significant non-specific hybridization to the control probes was observed at room temperature (data not shown) the hybridization temperature was set at 37 °C. Then, to detect *L. pneumophila* with high specificity and in very low concentrations, the effect of experimental parameters, namely the buffer composition, the length of the spacer between detector probe and biotin, and the pre-treatment of 16s rRNA were investigated.

3.1. Effect of buffer composition and detector probe spacer on hybridization efficiency

In addition to the hybridization temperature, the buffer composition and the proximity between the detection probe and its respective biotin functional group also play an important role in the stringency and efficiency of the hybridization (Bockisch et al., 2005; Small et al., 2001).

A 60 bp synthetic RNA sequence was selected from *L. pneumophila's* 16s rRNA sequences complimentary to the Leg1 CP. Therefore, 60 bp synthetic RNA (Table S1) was utilized to investigate the effect of the buffer composition and the detector probe spacer.

The effect of buffer compositions on the SPRi differential reflectivity ($\Delta\%R$) of synthetic RNA hybridization for an incubation time of 18 min is illustrated in Fig. 1. To better compare the different buffer compositions, the signals obtained from the control probes were subtracted from the Leg1 CP hybridization signals at each buffer composition (Fig. 1 inset). Increasing the salt concentrations by four-fold (from 150 mM to 600 mM) resulted in higher hybridization efficiency. A further increase of the salt concentration to 900 mM showed a slight increase in hybridization efficiency but caused an increase in non-specific adsorption to the control probe. Thus, 600 mM SSPE was set as the optimal hybridization buffer. As for the optimal biotinylated spacer, different spacers, such as dT and TEG (containing a 15C spacer), were investigated, whereas TEG yielded the highest signal (data not shown). These optimized hybridization parameters were then set for the detection of 16s rRNA in further investigations.

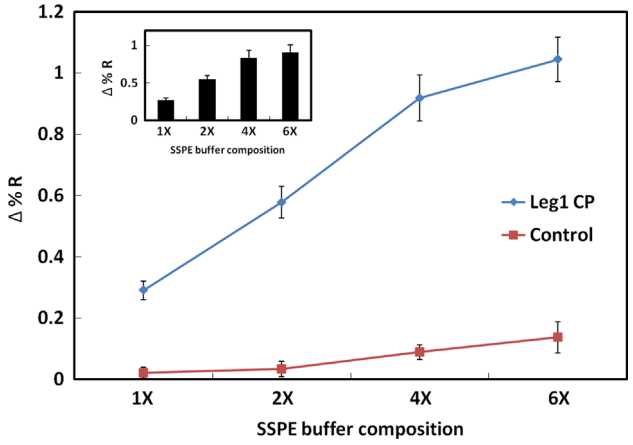

Fig. 1. Effect of buffer composition on hybridization efficiency. Hybridization of 10 nM synthetic RNA for 18 min on the biochip expressed as $\Delta\%R$ as a function of buffer composition (1 × –6 × SSPE). The inset represents the difference between the hybridization signal of the Leg1 CP and that of the control probes. All data is expressed as mean ± standard deviation ($n=5$).

3.2. L. pneumophila 16s rRNA pre-treatment

Conversely, to address the steric hindrance resulting from the secondary structure of 16s rRNA, the effect of different pre-treatment methods was investigated. Fig. 2a shows the changes in SPRi differential reflectivity signals representing 18-minute hybridization for pre-treated, as well as intact, 16s rRNA to the Leg1, Leg2 and EU CPs.

In general, Leg1 CP produced stronger hybridization signals compared to the Leg2 and EU capture probes. This may be attributed to several factors, including: (i) the higher melting temperature of Leg1 CP compared to the Leg2 and EU CPs, (ii) the position of the Leg1 CP complementary sequence, located on the more exposed region of the 16s rRNA secondary structure, and (iii) the weaker secondary structure of 16s rRNA to be disrupted by the Leg1 CP compared to the Leg2 and EU capture probes (Fig.3a and b). To arrive at the optimized fragmentation protocol, two methods with varying fragmentation solution concentrations were used to obtain the 16s rRNA fragments, referred to as Frag1 and Frag2. As shown in Fig. 2a, denaturation through heating of the 16s rRNA resulted only in a significant increase of $\Delta\%R$ for hybridization to EU CP, but not Leg1 and Leg2 CPs. The same trend was also observed for Frag1. In addition, Frag2 resulted in the highest improvement in hybridization efficiency among the three capture probes relative to intact 16s rRNA. This is due to the higher concentration of cations in Frag2 compared to those in Frag1, which results in smaller fragments and, in turn,

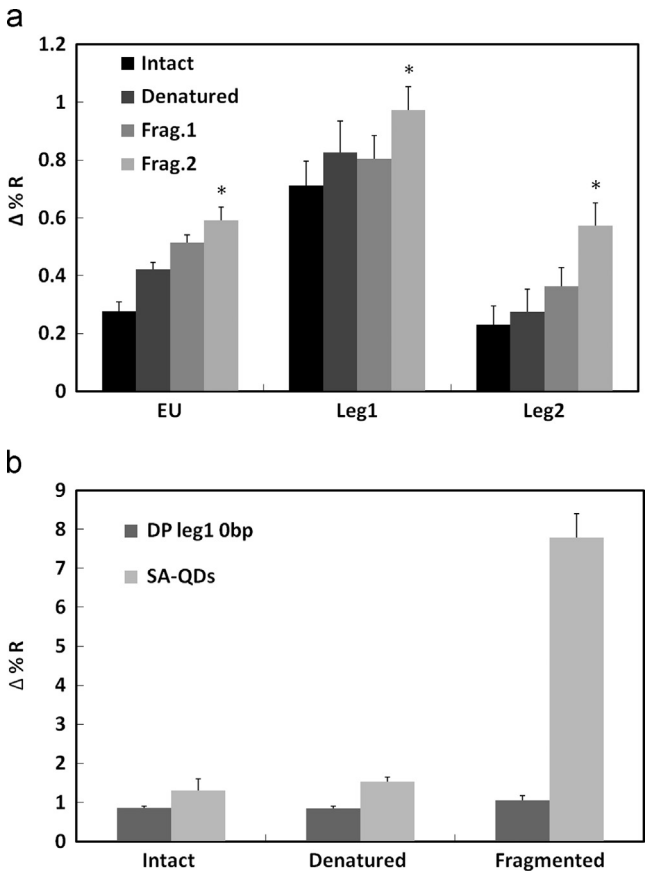

Fig. 2. Effect of fragmentation and denaturation pre-treatment methods on 16s rRNA on hybridization efficiency. (a) Hybridization of 10 nM 16s rRNA after 18 min incubation with EU, Leg1 and Leg2 capture probes. (b) Effect of 16s rRNA pre-treatment on QDs post amplification. 100 nM Leg1 DP 0 bp with 10 nM 16s RNA were used and hybridization efficiency with Leg1 CP followed by addition of the 1 nM SA-QDs was investigated. All data is expressed as mean + standard deviation ($n=5$, $^*P<0.05$ versus intact, denatured and Frag1).

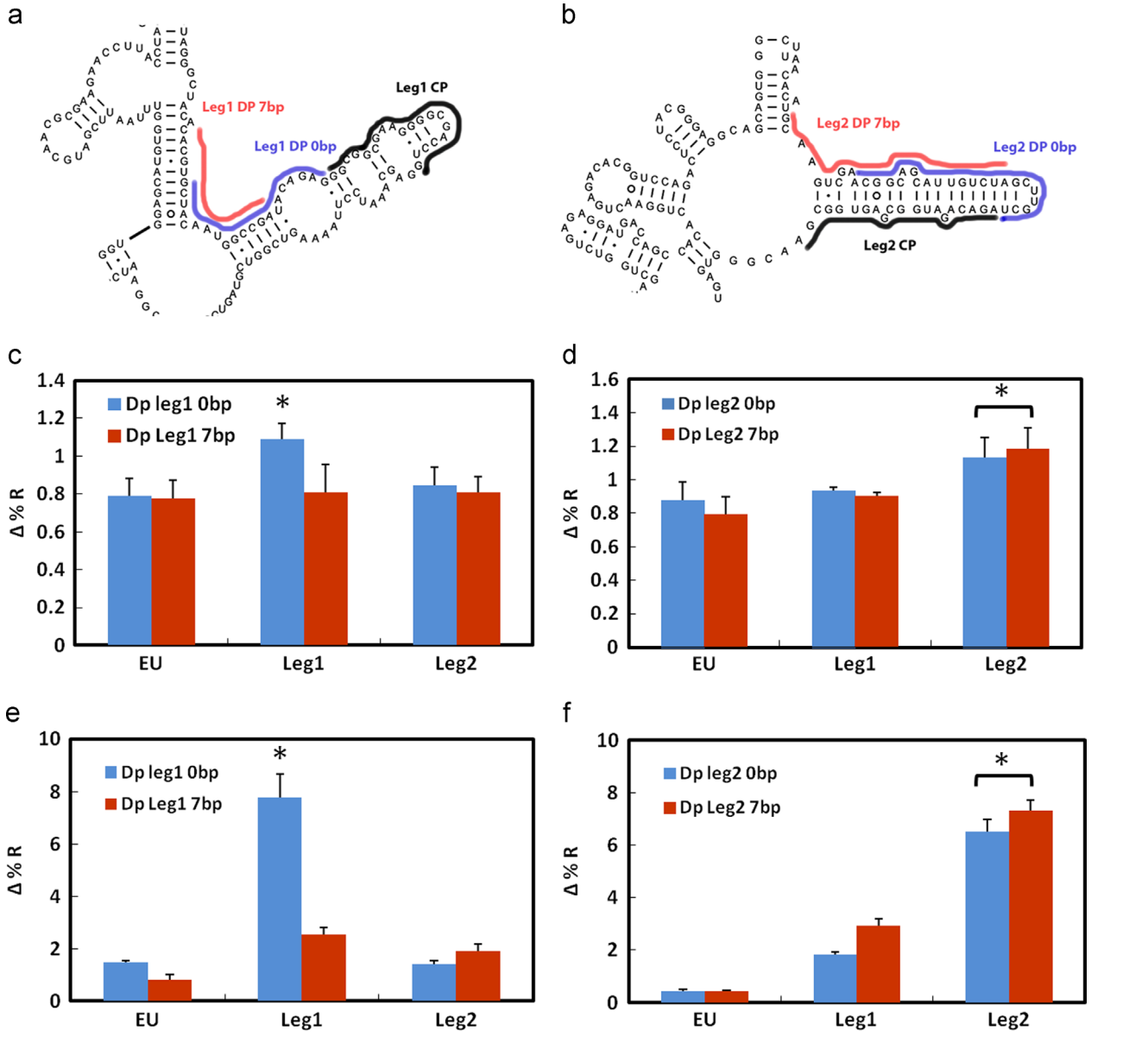

Fig. 3. Effect of different detector probes on hybridization efficiency. *x*-axis represents capture probes. (a,b) Secondary structure diagrams for *Legionella pneumophila* based on *L. pneumophila* model (accession number M34113) (Cannone et al., 2002) for area complementary to Leg1 CP and Leg2 CP respectively. Lines next to the diagrams indicate the position of capture and detector probes. (c,d) Change in reflectivity was measured after 18 min for three different capture probes (EU, Leg1 and Leg2 CPs) for 10 nM fragmented 16s rRNA corresponding to a and b respectively. (e,f) Addition of 1 nM SA-QDs for 10 min corresponding to c and d respectively. All data is expressed as mean + standard deviation ($n=5$, $^{*}P<0.05$ versus other capture probes).

higher accessibility of the capture probes. For simplicity's sake, fragmentation will henceforth refer to Frag2.

To further investigate the effect of pre-treatment of the 16s rRNA, biotinylated detector probes located 0 bp away from the Leg1 CP were investigated for hybridization efficiency and subsequent signal amplification through the addition of SA-QDs. Leg1 DP 0 bp was pre-mixed with fragmented, denatured, and intact 16s rRNA samples before injection into the SPRi system. Fig. 2b shows the Δ%*R* for hybridization, using Leg1 CP, of 16s rRNA pre-mixed with Leg1 DP 0 bp for 18 min, followed by the addition of SA-QDs and a 10 min reaction time, as a function of the pre-treatment methodology. Addition of the detector probe resulted in a slight increase in the signal, with the highest for fragmented 16s rRNA. SA-QDs addition also resulted in a drastic change in Δ%*R* for fragmented 16s rRNA versus slight signal enhancement for intact and denatured RNAs. The enhanced hybridization efficiency could be explained by a higher number of hybridized detector probes for fragmented RNA due to the easy access of smaller RNA as well as the ease of access of SA-QDs to the small 16s rRNA fragments compared to the whole 16s rRNA.

3.3. Determination of the SPRi limit of detection for 16s rRNA from *L. pneumophila*

The optimal experimental parameters, the pre-treatment fragmentation, and the SA-QD post amplification strategy were used to investigate two more critical factors, the distance between the capture and the detector probe and the hybridization time, affecting the specificity and efficiency of the target sequence hybridization extracted from *L. pneumophila* and to determine the SPRi limit of detection (LOD) (Small et al., 2001).

To investigate the effect of the detector probe's proximity to the capture probe on the specificity and sensitivity of the detection system, two detector probes for the Leg1 and Leg2 capture probes

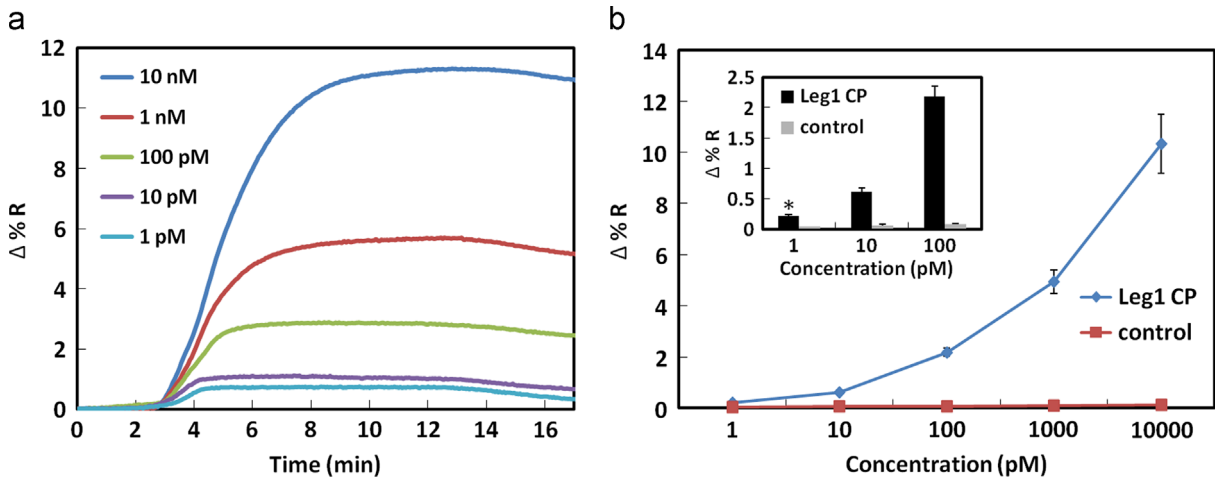

Fig. 4. Fragmented 16s rRNA hybridization with Leg1 CP with series of ultralow RNA concentrations: 10 nM, 1 nM, 100 pM, 10 pM, 1 pM. (a) Normalized real-time SPRi kinetic curve for detection of ultralow concentration of 16s rRNA. (b) The reflectivity change was plotted versus concentration after 150 min. The inset figure shows the differential reflectivity change ($\Delta\%R$) for 1 pM, 10 pM and 10 pM. All data expressed as mean ± standard deviation ($n=5$,*$P<0.05$ versus control probe).

were designed to hybridize to the 16s rRNA sequence 0 and 7 bp away from the respective capture probes (Fig. 3a and b). Fig. 3c–f shows the hybridization of four detector probes with fragmented 16s rRNA along with the use of SA-QD signal amplification for incubation times of 18 and 10 min, respectively. The results indicated that Leg2 CP possessed a higher signal when Leg2 DPs (Leg2 DPs at 0 and 7 bp) were used compared to Leg1 DPs (Leg1 DPs at 0 and 7 bp) (Fig. 3c and d). This was further accentuated after the addition of SA-QDs. Both Leg2 DPs produced significantly higher signals compared to Leg1 DPs (Fig. 3e and f). This could be due to the position of these probes on the secondary structure of 16s rRNA. As shown in Fig. 3b, Leg2 CP and Leg2 DPs target the same stem-loop in the 16s rRNA secondary structure. The presence of Leg2 DPs, therefore, causes disruption of this stem-loop and further facilitates the reaction with Leg2 CP.

The same hybridization trend was therefore expected for Leg1 CP with both Leg1 DPs. However, only Leg1 DP 0 bp showed a markedly enhanced signal either with 16s rRNA hybridization or the following SA-QD post amplification. Further examination of the secondary structure of *L. pneumophila* revealed that the position of Leg1 DP 0 bp and Leg1 DP 7 bp contributes significantly to this difference. As shown in Fig. 3a, Leg1 DP 0 bp contains two internal loops compared to Leg1 DP 7 bp, which possesses only one internal loop. Upon further examination of the secondary structure, it was apparent that, for Leg1 DP 7 bp hybridize to 16s rRNA, it needs to overcome a stronger secondary structure compared to Leg1 DP 0 bp (14 bonds compared to 9). Since the Leg1 DP 0 bp produced the most pronounced SPRi signal, it was selected for further experiments.

Finally, to determine the effect of hybridization time, fixed volumes of fragmented 16s rRNA were used with incubation times ranging from 4.5 min to 150 min, obtained by varying the flow rate to the SPRi system. The range of incubation was purposely selected to maintain the time of analysis comparable to that of PCR. Fig. S1 presents the effect of hybridization time on $\Delta\%R$ for Leg1 CP. As expected, increased incubation time was directly related to enhanced hybridization efficiency.

An incubation time of 150 min was then chosen, along with optimal hybridization conditions, to investigate the SPRi sensitivity and its LOD for the detection of 16s rRNA from *L. pneumophila*. 16s rRNA hybridization with multiple samples containing fragmented 16s rRNA varying in concentration from 1 pM to 10 nM, with 100 nM Leg1 DP 0 bp in 4 × SSPE buffer were taken, and the hybridization adsorption kinetics were monitored in real time with SPRi measurements employing the SA-QD signal amplification strategy. The normalized SPRi kinetic curves for SA-QD adsorption for various 16s rRNA concentrations ranging from 1 pM to 10 nM are given in Fig. 4a. Fig. 4b shows the plot of the $\Delta\%R$ for Leg1 and control capture probes for the aforementioned concentrations. The inset in Fig. 4b shows the $\Delta\%R$ for low concentrations of 16s rRNA (1,10, and 100 pM). A significant difference in the SPR signal was observed between Leg1 CP and the control probe even at 1 pM 16s rRNA, which clearly established a limit of detection on the order of 1 pM *L. pneumophila* 16s rRNA. This value could be translated to the equivalent of 88.5 CFU μL^{-1} with the assumption of 6800 ribosomes per bacteria (Leskelä et al., 2005). This limit of detection is far lower than the previously reported value for RNA detection using an SPR biosensing system (Joung et al., 2008; Nelson et al., 2000).

4. Conclusions

Developing a detection system that distinguishes metabolic active pathogens with the desired specificity, sensitivity, and time of detection is of great importance and relevance for the rapid detection of pathogens in environmental samples. In this paper, we conclusively demonstrated that a sub-femtomole level of 16s rRNA from pathogenic *L. pneumophila* can be specifically detected using an optimized experimental protocol, adequate design of capture and detector probes, and employing a QD signal amplification strategy with a SPRi biosensor. The proposed approach offers several distinct advantages compared to other conventional detection systems, including high specificity through the design of two probes (capture and detector) for the target, high sensitivity through using QD signal post amplification, and rapid and reliable quantification using *L. pneumophila's* 16s rRNA, which is a good representation of metabolically active bacteria.

To achieve specific and sensitive detection, optimal hybridization conditions and parameters were implemented. We showed that the SPRi detection of 16s rRNA in solutions as diluted as 1 pM at 500 μL (0.5 femtomole) can be achieved in less than three hours, making the SPRi detection system suitable for the direct detection of *L. pneumophila*, in man-made water systems. Through the integration of a microfluidic system with SPRi and further automation, it would be possible to reduce further the detection volume to less than 1 μL and improve the LOD significantly.

Acknowledgments

We acknowledge National Science and Engineering Research Council of Canada-Collaborative Research program and Discovery program, Genome Canada/Genome Quebec, Nano-Quebec and Le Fonds Quebécois de la Recherche sur la Nature et les Technologies-Centre for Biorecognition and Biosensors for their financial support. The authors would also like to thank Dr J.-J. Drieux and Dr P. Hiernaux from Magnus for their technical support and advice, S. Shapka and S. Filion-Côté for scientific discussions regarding SPRi and Dr T. Fatanat Didar for his comments on the manuscript. Work in SPF laboratory is supported by NSERC Discovery Grant 418289-2012.

Appendix A. Supporting information

Supplementary data associated with this article can be found in the online version at http://dx.doi.org/10.1016/j.bios.2013.08.032.

References

Bockisch, B., Grunwald, T., Spillner, E., Bredehorst, R., 2005. Nucleic Acids Research 33 (11), e101.
Cannone, J.J., Subramanian, S., Schnare, M.N., Collett, J.R., D'Souza, L.M., Du, Y., Feng, B., Lin, N., Madabusi, L.V., Müller, K.M., 2002. BMC Bioinformatics 3 (1), 2.
CDC, 2011. MMWR, 1083–1086.
Clarridge 3rd, J.E., 2004. Clinical Microbiology Reviews 17 (4), 840–862. (table of contents).
Coenye, T., Vandamme, P., 2003. FEMS Microbiology Letters 228 (1), 45–49.
Elsholz, B., Worl, R., Blohm, L., Albers, J., Feucht, H., Grunwald, T., Jurgen, B., Schweder, T., Hintsche, R., 2006. Analytical Chemistry 78 (14), 4794–4802.
Foudeh, A.M., Fatanat Didar, T., Veres, T., Tabrizian, M., 2012. Lab on a Chip 12 (18), 3249–3266.
Gerasimova, Y.V., Kolpashchikov, D.M., 2012. Biosensors and Bioelectronics, 0).
Hwang, K.-Y., Jeong, S.-Y., Kim, Y.-R., Namkoong, K., Lim, H.-K., Chung, W.-S., Kim, J.-H., Huh, N., 2011. Sensors and Actuators B: Chemical 154 (1), 46–51.
Joung, H.-A., Lee, N.-R., Lee, S.K., Ahn, J., Shin, Y.B., Choi, H.-S., Lee, C.-S., Kim, S., Kim, M.-G., 2008. Analytica Chimica Acta 630 (2), 168–173.
Lazcka, O., Campo, F.J.D., Muñoz, F.X., 2007. Biosensors and Bioelectronics 22 (7), 1205–1217.
Leskelä, T., Tilsala-Timisjärvi, A., Kusnetsov, J., Neubauer, P., Breitenstein, A., 2005. Journal of Microbiological Methods 62 (2), 167–179.
Malic, L., Sandros, M.G., Tabrizian, M., 2011. Analytical Chemistry 83 (13), 5222–5229.
McKillip, J.L., Jaykus, L.-A., Drake, M., 1998. Applied and Environmental Microbiology 64 (11), 4264–4268.
Nelson, B.P., Grimsrud, T.E., Liles, M.R., Goodman, R.M., Corn, R.M., 2000. Analytical Chemistry 73 (1), 1–7.
Nygård, K., Werner-Johansen, Ø., Rønsen, S., Caugant, D.A., Simonsen, Ø., Kanestrøm, A., Ask, E., Ringstad, J., Ødegård, R., Jensen, T., Krogh, T., Høiby, E.A., Ragnhildstveit, E., Aaberge, I.S., Aavitsland, P., 2008. Clinical Infectious Diseases 46 (1), 61–69.
Oh, B.K., Kim, Y.K., Lee, W., Bae, Y.M., Lee, W.H., Choi, J.W., 2003. Biosensors and Bioelectronics 18 (5-6), 605–611.
Riahi, R., Mach, K.E., Mohan, R., Liao, J.C., Wong, P.K., 2011. Analytical Chemistry 83 (16), 6349–6354.
Small, J., Call, D.R., Brockman, F.J., Straub, T.M., Chandler, D.P., 2001. Applied and Environmental Microbiology 67 (10), 4708–4716.
Stephen, K.E., Homrighausen, D., DePalma, G., Nakatsu, C.H., Irudayaraj, J., 2012. Analyst 137 (18), 4280–4286.
Swanson, M., Hammer, B., 2000. Annual Reviews in Microbiology 54 (1), 567–613.
Von Baum, H., Härter, G., Essig, A., Lück, C., Gonser, T., Embacher, A., Brockmann, S., 2010. Eurosurveillance 15 (4), 19472.
Wadowsky, R., Wilson, T., Kapp, N., West, A., Kuchta, J., Dowling, J., Yee, R., 1991. Applied and Environmental Microbiology 57 (7), 1950–1955.
WHO, 2003. pp. 1–24.
Xie, H., Zhang, C., Gao, Z., 2004. Analytical Chemistry 76 (6), 1611–1617.
Zhou, G., Wen, S., Liu, Y., Li, R., Zhong, X., Feng, L., Wang, L., Cao, B., 2011. International Journal of Food Microbiology 145 (1), 293–300.